Published in final edited form as:
Clin Cancer Res. 2008 March 1; 14(5): 1519–1528. doi:10.1158/1078-0432.CCR-07-4628.

Synergy of a Herpes OncolyticVirus and Paclitaxel for Anaplastic Thyroid Cancer

Shu-Fu Lin[1,4], **Sizhi Paul Gao**[2], **Daniel L. Price**[1], **Sen Li**[1], **Ting-Chao Chou**[3], **Paramjeet Singh**[1], **Yu-Yao Huang**[4], **Yuman Fong**[1], and **Richard J. Wong**[1]

[1]Department of Surgery, Memorial Sloan-Kettering Cancer Center, New York, New York

[2]Department of Medicine, Memorial Sloan-Kettering Cancer Center, New York, New York

[3]Department of Laboratory of Preclinical Pharmacology Core, Memorial Sloan-Kettering Cancer Center, New York, New York

[4] Division of Endocrinology and Metabolism, Department of Internal Medicine, Chang Gung Memorial Hospital, Taoyuan, Taiwan

Abstract

Purpose—Novel therapeutic regimens are needed to improve the dismal outcomes of patients with anaplastic thyroid cancer (ATC). Oncolytic herpes simplex virus have shown promising activity against human ATC. We studied the application of oncolytic herpes simplex virus (G207 and NV1023) in combination with currently used chemotherapeutic drugs (paclitaxel and doxorubicin) for the treatment of ATC.

Experimental Design and Results—All four agents showed dose-response cytotoxicity in vitro for the human ATC cell lines KAT4 and DRO90-1. G207, combined with paclitaxel, showed synergistic cytotoxicity. Chou-Talalay combination indices ranged from 0.56 to 0.66 for KAT4, and 0.68 to 0.74 for DRO90-1at higher affected fractions. Paclitaxel did not enhance G207 viral entry and early gene expression or G207 viral replication. Paclitaxel combined with G207 compared with single-agent treatment or controls showed significantly increased microtubule acetylation, mitotic arrest, aberrant chromatid separation, inhibition of metaphase to anaphase progression, and apoptosis. A single i.t. injection of G207 combined with biweekly i.p. paclitaxel injections in athymic nude mice bearing KAT4 flank tumors showed significantly reduced mean tumor volume (74 F 38 mm3) compared with G207 alone (388 F 109 mm3), paclitaxel alone (439 F 137 mm3), and control (520 F 160 mm3) groups at 16 days. There was no morbidity in vivo attributable to therapy.

Conclusions—Mechanisms of paclitaxel antitumoral activity, including microtubule acetylation, mitotic block, and apoptosis, were enhanced by G207, which also has direct oncolytic effects. Combination of G207 and paclitaxel therapy is synergistic in treating ATC and holds promise for patients with this fatal disease.

Anaplastic thyroid cancer (ATC) is one of the most aggressive human malignancies and is considered a fatal disease. ATC represents <2% of all thyroid cancers but is responsible for up to 40% of mortality from thyroid cancer (1). The median survival of patients with ATC is f6 months (1–3). Currently available chemotherapy drugs with activity against ATC include doxorubicin (Adriamycin), paclitaxel, and cisplatin. The response rate of ATC to Adriamycin is poor, and combination drug therapy fails to give an added benefit (4,5). Although response rates to paclitaxel were 53% in a recent phase II clinical trial, the median survival of those

Corresponding Author: Richard J.Wong, Head and Neck Service, C-1069, Department of Surgery, Memorial Sloan-Kettering Cancer Center, 1275 York Avenue, New York, NY 10021. Phone: 212-639-7638; Fax: 212-717-3302; E-mail: E-mail: wongr@mskcc.org.

patients responding to paclitaxel was only 32 weeks (6). Multimodality therapy for ATC, including surgical debulking, external radiation therapy, and chemotherapy, have failed to show any meaningful survival improvements from multimodality therapy (6–10). Novel therapies with different mechanisms of action are likely necessary to achieve any significant improvements in these dismal outcomes.

Attenuated, replication-competent herpes simplex virus type 1(HSV-1) have been engineered with significantly reduced toxic effects compared with wild-type HSV-1 (11,12). These attenuated viruses have shown efficacy in treating a variety of malignancies, including anaplastic thyroid cancer, in preclinical studies (11–17). G207 is attenuated by deletions of both copies of the diploid g134.5 neurovirulence gene and a lacZ gene insertion inactivating the ribonucleotide reductase (RR) gene (12). The NV series of viruses have a single deletion in g134.5, and NV1023 express lacZ (15,18). Early clinical trials have shown that these attenuated oncolytic viruses and others may be safe for clinical application at doses reaching up to 1.3 × 109 plaque-forming units (pfu; refs. 19–21).

Oncolytic herpes viruses have been applied in combination with chemotherapy in preclinical studies to potentially increase treatment efficacy for various malignancies (22–28). Several studies have suggested that G207, in combination with DNA damaging agents, such as fluorodeoxyuridine, mitomycin C, and temozolomide, may have synergistic antitumoral effects (26–28). GADD34, a DNA repair enzyme, shares close homology to HSV-1 g134.5, which is deleted for purposes of neurovirulence attenuation. Selected chemotherapy agents that up-regulate cellular GADD34 in response to DNA damage may potentially complement the g134.5 deletion in G207 to enhance viral proliferation and oncolytic efficacy (26–28). However, studies investigating the mechanistic interactions between oncolytic HSV and chemotherapy used for ATC, such as Adriamycin and paclitaxel, have not previously been reported.

Our group has shown that oncolytic herpes viruses may have potent therapeutic effects in treating anaplastic thyroid cancer in vitro and in animal models (16,29). The purpose of the current study is to investigate the potential application of oncolytic HSV (G207 or NV1023) in combination with chemotherapy for ATC to assess for beneficial interactions. Adriamycin inhibits the activity of topoisomerase II causing breaks in genomic DNA and may also increase the R2 protein of RR (30,31). Paclitaxel causes microtubule stabilization, mitotic arrest, and apoptosis in cancer cells (32,33). We sought to determine if G207 or NV1023 might show enhanced effects with either Adriamycin or paclitaxel, possibly through alterations in cellular GADD34 or RR.

The combination of oncolytic herpes virus (G207 or NV1023) with chemotherapy (Adriamycin or paclitaxel) was studied in two human ATC cell lines (KAT4 or DRO90-1) by cytotoxicity assays. Combination cytotoxic effects were assessed using Chou-Talalay multiple drug effect analyses (34). The combination of G207 with paclitaxel showed synergistic effects for both cell lines. The potential mechanisms of these antitumoral effects were assessed by viral entry and early gene expression assays, proliferation plaque assays, acetylated atubulin detection, determination of mitotic arrest, assessment of metaphase-to-anaphase transition, and apoptosis assays. Athymic nude mice with ATC flank tumors were treated with i.t. G207 plus i.p. paclitaxel to confirm the efficacy of combination treatment in vivo and to evaluate for safety. These results show that G207 viral entry and replication is not enhanced by paclitaxel therapy. G207 causes direct viral oncolysis while also enhancing the mechanism of paclitaxel activity by increasing a-tubulin acetylation, stabilizing microtubules, inducing mitotic arrest, inhibiting metaphase-to-anaphase progression, and increasing apoptosis. This study shows that the combination of G207 and paclitaxel has synergistic antitumoral effects for ATC.

Materials and Methods

Cell lines

Two human ATC cell lines were obtained. KAT4 was a gift of Dr. K. Ain (University of Kentucky Medical Center). DRO90-1 was a gift of Dr. G. Juillard (University of California). KAT4 and DRO90-1were maintained in RPMI with 14 mL/L nonessential amino acid, L-glutamine (100 mg/L), sodium pyruvate (154 mg/L), and sodium bicarbonate (1.5 g/L). African green monkey kidney cells (Vero cells) for viral plaque assays were maintained in MEM. All media contained 10% FCS, 100,000 units/L penicillin, and 100 mg/L streptomycin. All cells were maintained in a 5% CO2 humidified incubator at 37jC.

Viruses

G207 is an attenuated, replication competent, mutant HSV-1with deletions at both g134.5 loci and a *lacZ* gene insertion inactivating the ICP6 gene (RR), whose construction has been previously described (12). NV1023 is an attenuated, replication competent HSV-1, whose construction has also been previously described (15). NV1023 contains a fragment of HSV-2 DNA inserted in UL/S junction, a deletion of UL56, and one copy of the diploid genes ICP0, ICP4, and g134.5. NV1023 contains the lacZ gene inserted at the US10–12 locus. Both viruses were obtained from Medigene. Viruses were diluted with serum-free media for in vitro studies and with PBS for in vivo studies.

Chemotherapy

Paclitaxel and Adriamycin were obtained from Sigma Chemical Co. Paclitaxel was diluted in DMSO (tissue culture grade; Sigma) and added to media for a final concentration of DMSO of <0.1% (v/v) for in vitro studies. For in vivo studies, paclitaxel was dissolved in cremophor EL (Sigma) and dehydrated ethanol (1:1 v/v) to a concentration of 30 mg/mL and stored at −20jC. Before i.p. injections, paclitaxel was diluted in 0.9% saline to a final concentration of 4 mg/mL. Adriamycin was diluted with 0.9% saline before in vitro use.

Cytotoxicity assays and Chou-Talalay analysis

KAT4 and DRO90-1 cytotoxicity resulting from virus, chemotherapy, or both agents in combination was studied using lactate dehydrogenase (LDH) assays. Cells were plated at 2×10^4 cells per well in 12-well plates in 1 mL media. After overnight incubation, the agent or vehicle was added at the indicated concentration. Serial dilutions were tested starting at the following starting doses: G207 at multiplicity of infection (MOI) of 8, NV1023 at MOI of 1, paclitaxel at 32 nmol/L, and Adriamycin at 6.4 Amol/L over a 4-day time course. After initial studies designed to select appropriate dose ranges, additional LDH assays were done to generate dose-response curves assessed at day 4. Median effect doses (D_m) were calculated for each cell line and each drug.

For combination studies, LDH cytotoxicity assays of G207 + paclitaxel, G207 + Adriamycin, NV1023 + paclitaxel, and NV1023 + Adriamycin at a fixed dose ratio were done on day 4 after treatment. Cells were washed with PBS and lysed with Triton X (1.35%; Sigma) to release intracellular LDH, which was quantified with a Cytotox 96 kit (Promega) at 450 nm by spectrophotometry (EL321e, Bio-Tek Instruments). Results are expressed as the percentage of surviving cells determined by comparing the LDH of each sample relative to control samples considered 100% viable. The dose-response curves of each agent for each cell line were obtained. The interactions between viruses and drugs were evaluated by calculating Chou-Talalay combination indices (CI) using CompuSyn software (ComboSyn). Each condition was replicated in triplicate, and each experiment was done at least twice to corroborate results.

Viral entry

G207 expresses the h-galactosidase gene as a marker of infection and gene expression. Cells were plated at 2×10^4 per well in 96-well plates and then exposed to paclitaxel at varying doses for 6 h. For DRO90-1, serial dilutions from 24 nmol/L were done, whereas for KAT4, serial dilutions from 16 nmol/L were done. Cells were then exposed to G207 at MOI of 5. After 6 h of incubation, cells were lysed and h-galactosidase activity was measured with an Enhanced h-Galactosidase Assay kit (Gene Therapy Systems) and spectrophotometry (EL321e, Bio-Tek Instruments) at 570 nm. All conditions were measured in triplicate.

Viral titering

Viral proliferation was measured by plating 2×10^4 cells in 12-well plates overnight and then treating them with G207 at MOI of 0.5 (KAT4) or MOI of 1.5 (DRO90-1) and paclitaxel 1 nmol/L (KAT4) or 3 nmol/L (DRO90-1) or DMSO as a control. Cells were scraped and collected daily with supernatants for 4 days. Three freeze-thaw cycles were done to release intracellular virus, and serial dilutions of the samples were done. Diluted samples were added to plates of confluent Vero cells for standard viral plaque assays (26). All conditions were measured in triplicate. For studies calculating the ratio of viral pfu per viable cancer cell, cells were treated for 2 days with G207 (MOI, 1) and a range of paclitaxel doses, and the number of viable cells was counted from additional wells.

Western blots

KAT4 cells were plated at 2×10^5 cells in 100-mm Petri dishes in 10 mL media overnight and treated with G207 at MOI of 1, 2 nmol/L paclitaxel, both, or neither for 48 and 72 h. Cell pellets were treated with lysis buffer (Cell Signaling Technology), protease inhibitor mixture (Complete Mini EDTA-free, Roche), sonicated, and clarified by centrifugation. Total protein (25 Ag) was electrophoresed on 10% Tris-HCl gels (Bio-Rad), transferred to polyvinylidene difluoride membranes, blocked, and exposed to a mouse monoclonal acetylated a-tubulin primary antibody (6-11B-1, 1:2,000; Sigma) or mouse a-tubulin antibody (B-5-1–2, 1:8,000; Sigma) followed by a secondary antibody conjugated to horseradish peroxidase. Signal was developed using an Enhanced Chemiluminescence Plus Detection System (Amersham). Band density was quantified (AlphaImager Imaging Systems), and the ratio of acetylated atubulin to a-tubulin was divided by control to yield relative protein expression.

Immunofluorescence microscopy

KAT4 cells were plated at 2×10^4 in four-well culture slides in 1mL media overnight. Cells were treated with the indicated agents for 72 h, fixed in 100% dehydrated ethanol or methanol/acetone 1:1 (5 min, −20jC), washed with PBS, blocked with 1% bovine serum albumin/PBS (10 min, 37jC), and incubated with a mouse a-tubulin antibody (B-5-1–2, 1:2,000; Sigma) or mouse acetylated a-tubulin antibody (6-11B-1, 1:400; Sigma) for 25 min at 37jC. Cells were then washed in PBS and incubated with a secondary AlexaFluor 633-conjugated goat antimouse antibody (1:500; Molecular Probes) or AlexaFluor 488– conjugated goat anti-mouse antibody (1:1,000; Molecular Probes) for 25 min at 37jC. Cells were then washed with PBS, incubated with 4¶,6-diamidino-2-phenylindole (DAPI; 0.2 Ag/mL; Invitrogen) for 10 min at room temperature, washed again with PBS, and covered with VECTASHIELD Mounting Media (Vector Laboratories). Images were captured with a Leica TCS SP2 AOBS confocal microscope (Leica Microsystems). For mitotic index assessment, a minimum of 1,500 cells were counted from at least five different fields for each condition. Anaphase/metaphase ratio was evaluated by counting a minimum of 180 mitotic cells from three different fields for each condition.

Apoptosis assay

KAT4 cells were plated at 2×10^5 cells per dish in 60-mm dishes in 5 mL medium overnight. Vehicle, G207 (MOI, 0.5), paclitaxel (4 nmol/L), or a combination of G207 with paclitaxel was added. After 72 h, floating cells were collected and combined with trypsinized, adherent cells. Samples were washed with 1mL 1% bovine serum albumin/PBS and fixed with 70% ethanol at 4jC overnight. Cells were then washed with 1mL of 1% bovine serum albumin/PBS and treated with RNase A (100 Ag/mL; Sigma) and propidium iodide (5 Ag/mL; Sigma) at 37jC for 15 min. Apoptotic cells were characterized by subdiploid DNA content as detected by flow cytometry on a FACScalibur cytometer (Becton Dickinson), and data were analyzed by FlowJo v8.5.3 software (Tree Star). All samples were replicated in triplicate.

Flank tumor therapy

Six-week-old athymic female nude mice (National Cancer Institute) were anesthetized with inhalational isoflurane (Baxter). KAT4 flank tumors were established by injecting 1×10^6 cells in 100 AL PBS into the s.c. flanks of athymic nude mice. When tumors had reached f4 to 5 mm in mean diameter, mice (n = 4 per group) were treated with a single dose of G207 (2 _ 107 pfu/50 AL) or PBS by i.t. injection. Paclitaxel (0.4 mg/100 AL) or vehicle (cremophor EL/ dehydrated ethanol/saline) was given by i.p. injection after the G207 injection. Paclitaxel or vehicle was injected i.p. on days 1and 4 of a 7-day cycle for 2 weeks. Tumor dimensions were serially measured with electronic calipers every 2 days, and the volumes were calculated by the following the formula $a^2 \times b \times 0.4$, where *a* represents the smallest diameter and *b* is the perpendicular diameter. The tumor volumes ± SEs of the mean were reported. The body weight and motor activity of each animal were monitored as indicators of general health.

Statistical analysis

The statistical significance of differences between two groups was assessed when appropriate, using two-sided Student's *t* test with $P < 0.05$. Results are expressed as the mean ± SE.

Results

In vitro cytotoxicity of paclitaxel, Adriamycin, NV1023, G207

DRO90-1and KAT4 both showed dose-dependent cytotoxicity over a 4-day time course after exposure to paclitaxel, Adriamycin, NV1023, or G207 (Fig. 1). KAT4 was slightly more sensitive than DRO90-1 to paclitaxel cytotoxicity over the range of doses tested (32-2 nmol/ L). DRO90-1 was more sensitive than KAT4 to Adriamycin at higher doses (6.4-0.2 Amol/L), although DRO90-1was less sensitive at the lowest dose tested (0.1 Amol/L). KAT4 was slightly more sensitive to both NV1023 and G207 cytotoxicity than DRO90-1. Using results from these initial time course cytotoxicity experiments, new ranges of drug or viral doses were selected for dose response cytotoxicity studies done at day 4 (not shown). These data were used to calculate the median effect doses (D_m), causing 50% cytotoxicity for each agent. The D_m of paclitaxel was 0.89 nmol/L (KAT4) and 7.04 nmol/L (DRO90-1). The D_m of Adriamycin was 0.14 Amol/L (KAT4) and 0.15 Amol/L (DRO90-1). The D_m of G207 was MOI of 2.0 (KAT4) and MOI of 5.4 (DRO90-1). The D_m of NV1023 was MOI of 0.3 (KAT4) and MOI of 1.0 (DRO90-1).

Combination chemotherapy and viral cytotoxicity in vitro

To explore potential interactions between oncolytic HSV and chemotherapy for the treatment of ATC, cytotoxicity of G207 or NV1023 in combination with paclitaxel or Adriamycin was assessed in KAT4 and DRO90-1cell lines in vitro (Fig. 2). The greatest cytotoxicity was identified for the combination of G207 and paclitaxel, particularly at moderate and higher doses. The other combinations of virus and chemotherapy drug seemed to have less favorable

interactions. Potential interactions between virus and drug were evaluated using Chou-Talalay equations. A CI of <0.9 is considered synergistic, a CI between 0.9 and 1.1 is considered additive, and a CI of >1.1 is considered antagonistic (34). For the combination of G207 and paclitaxel, Chou-Talalay CIs ranged from 0.56 to 0.66 for KAT4 and 0.68 to 0.74 for DRO90-1 at higher affected fractions (Fa, >0.5), demonstrating synergistic cytotoxicity (Fig. 2B). The identification of synergy at higher affected fractions, meaning at higher overall cytotoxicity from combined therapy, is clinically relevant as effective treatment would necessitate higher combination doses.

The combination of NV1023 and paclitaxel was minimally synergistic (CI, 0.87-0.81) for KAT4 at higher affected fractions and was additive (CI, 0.85–0.97) for DRO90-1. Interestingly, we found that combination viral therapy with Adriamycin was additive (with G207) or antagonistic (with NV1023), but not synergistic at any conditions. The calculated dose reduction index is an indicator of the potential comparable reduction of drug dose achieved by its interaction with another agent. The greatest dose reduction indices were calculated for paclitaxel in combination with G207 at the higher affected fractions (Fig. 2C). Based on these findings, we focused on exploring interactions between G207 and paclitaxel.

Effects of paclitaxel on G207 viral entry and viral proliferation

The effect of paclitaxel on G207 entry into anaplastic thyroid cancer cells was assessed by lacZ assays (Fig. 3A). Low doses of paclitaxel seemed to modestly impair G207 entry and early gene expression, although at doses higher than 3 nmol/L this effect stabilized for both DRO90-1and KAT4. G207 viral entry was not enhanced by paclitaxel at any of the concentrations tested, suggesting that this is not a mechanism to account for synergistic interactions.

To determine if paclitaxel affects G207 viral replication in anaplastic thyroid cancer, viral replication was measured by plaque assays after infection with G207 and exposure to either paclitaxel or vehicle. Relatively low doses of paclitaxel were chosen to avoid overriding cytotoxicity impairing viral replication. A time course study showed no significant effects of paclitaxel on G207 viral replication (Fig. 3B). To assess for viral replication across a range of paclitaxel doses and to also account for alterations in viable cell numbers due to expected cytotoxicity from both paclitaxel and G207, we did additional viral titering studies at a set time point (day 2) and adjusted viral titers by viable cell number. The calculated numbers of viral pfu per viable cell did not significantly change across the range of paclitaxel doses tested for DRO90-1or KAT4 (Fig. 3C). Collectively, these data show that paclitaxel does not enhance G207 viral entry or viral replication.

Effects of G207 and paclitaxel on microtubule acetylation

We sought to determine if G207 may affect mechanisms of paclitaxel antitumoral activity. Paclitaxel is known to enhance microtubule stability, leading to mitotic arrest and, ultimately, apoptosis. The acetylation of a-tubulin is an established marker of microtubule stability, and the amount of acetylated tubulin is proportional to the stability of the microtubule (35). Quantitative Western blots were done to assess acetylated a-tubulin in KAT4 cells 48 and 72 h after treatment with vehicle, G207, paclitaxel, or G207 + paclitaxel. Treatment with paclitaxel alone led to relative increases in acetylated a-tubulin by 1.4-fold by 48 h and 2.4-fold by 72 h compared with untreated controls. Paclitaxel in combination with G207 led to much greater increases in acetylated α-tubulin of 2.9-fold by 48 h and 6.3-fold by 72 h (Fig. 4A and B).

Effects of G207 and paclitaxel on mitotic arrest and anaphase/metaphase ratio

The acetylation of α-tubulin and the increase in microtubule stability by paclitaxel leads to mitotic arrest and impaired progression of cells from metaphase to anaphase (33,36).

Immunofluorescence microscopy for α-tubulin and DAPI in KAT4 cells was done to assess the effects of G207 on paclitaxel-induced mitotic arrest and on metaphase-to-anaphase transition. The percentage of cells identified in mitosis was significantly increased for combination of G207 and paclitaxel treatment compared with paclitaxel alone or G207 alone (Fig. 4C). We also examined the ratio of cells in anaphase (segregated chromatids along microtubule spindles) to those at metaphase (lined up at metaphase plate) to determine whether progression between these phases of mitosis was blocked. A low ratio is a marker of microtubule stabilization by paclitaxel (36). The ratio was 0.22 ± 0.05 for control, 0.17 ± 0.03 for G207, 0.14 ± 0.02 for paclitaxel, and 0.07 ± 0.01for the combination of G207 with paclitaxel treatment (Fig. 4D). Therefore, the combination of G207 with paclitaxel was associated with a significantly higher mitotic arrest and a significantly lower anaphase-to-metaphase ratio compared with either paclitaxel or G207 alone ($P < 0.05$ for all comparisons, t test).

Apoptosis assay

We assessed the percentage of KAT4 cells undergoing apoptosis 72 h after treatment with G207 (MOI, 0.5), paclitaxel (4 nmol/L), G207 + paclitaxel, or vehicle as a control using propidium iodide staining and fluorescence activated cell sorting assessment of the sub-G_0 population of cells. The percentage of cells in apoptosis for control (1.4 ± 0.1%), G207 (14.5 ± 0.4%), paclitaxel (25.6 ± 0.8%), and combination of G207 and paclitaxel (33.9 ± 0.9%) was measured (Fig. 4E). The combination of G207 and paclitaxel showed a significant increase in apoptosis compared with either paclitaxel or G207 alone ($P < 0.01$for both comparisons, *t* test).

Immunofluorescence confocal microscopy

Immunofluorescence microscopy of KAT4 cells for acetylated tubulin shows a low level of fluorescence for control-treated and G207-treated KAT4 cells, mild fluorescence for paclitaxel-treated cells, and significantly enhanced fluorescence for G207 + paclitaxel–treated cells (Fig. 5A).

The morphologic changes of chromosomes for control-treated, G207-treated, paclitaxel-treated, and G207 + paclitaxel–treated KAT4 cells were assessed after DAPI (blue) and α-tubulin (red) immunofluorescence staining. For both control-treated and G207-treated cells, chromosomes retained a normal morphology throughout mitosis (Fig. 5B). The chromosomes line up in an organized fashion at the metaphase plate, and the sister chromatids are drawn uniformly apart by microtubules to opposing poles during anaphase. In contrast, some paclitaxel-treated cells show a failure by the chromosomes to congregate linearly along the metaphase plate. Others migrate in an aberrant fashion toward the opposing poles, with some chromosomes separate from the group. Most striking are the cells treated by the combination of G207 + paclitaxel. For these cells, we observed aberrant chromosomal morphology, fragmented portions of chromosomes, and mitotic catastrophes (Fig. 5B).

G207 and paclitaxel combination therapy of murine flank tumors

A flank tumor model of human KAT4 anaplastic thyroid cancer in athymic nude mice was used to study the effects of G207 and paclitaxel therapy in vivo. Groups with established flank tumors of equitable volumes were treated with vehicle, a single i.t. G207 injection, biweekly i.p. paclitaxel, or G207 + paclitaxel. KAT4 flank tumors receiving combination of G207 + paclitaxel showed a significantly reduced mean tumor volume (74 ± 38 mm^3) compared with G207 alone (388 ± 109 mm^3), paclitaxel alone (439 ± 137 mm^3), and control (520 ± 160 mm^3) by 16 days ($P < 0.01$ for all three comparisons; Fig. 6). Tumors treated with either G207 or paclitaxel alone had slightly smaller mean volumes than control group, but without statistical significance. The study was terminated when largest control group tumors began to ulcerate after day 16. The mean body weight of the mice was 22 g, and there were no significant differences between the groups initially or by the end of the study. The motor activity of all

the mice remained normal. There were no mucosal or cutaneous lesions identified on any animal. No morbidity attributable to either tumor progression or therapy was identified. No mortality was observed.

Discussion

Anaplastic thyroid cancer is one of the most aggressive human malignancies. Currently available treatments, including radiation therapy and chemotherapy, are considered palliative in nature. Novel therapies are needed to achieve improved outcomes for these unfortunate patients. Our group has previously reported on the preclinical efficacy of oncolytic herpes viruses for treating anaplastic thyroid cancers, using both in vitro assays and a murine in vivo animal model (16,29).

The combination of oncolytic herpes viral therapy with chemotherapy has been previously found to be effective for selected viruses and drugs (22–28). G207 acts mainly through direct viral oncolysis of infected cancer cells. One mechanism of synergy between chemotherapy and HSV oncolysis is related to the homology between GADD34, a DNA repair enzyme induced by some drugs, and $\gamma_1$34.5, a diploid neurovirulence HSV protein that may be deleted as an attenuation strategy. Drugs, such as temozolomide or mitomycin C, that stimulate GADD34 in cancer cells may also enhance herpes viral oncolysis by complementing the function of $\gamma_1$34.5 (27,28). RR is also deleted in certain oncolytic HSV-1, such as G207, as an attenuation strategy. Drugs, such as temozolomide and fluorodeoxyuridine, which can increase RR of a cancer cell may also enhance G207 viral replication and oncolysis (26,28). Selected chemotherapies may therefore potentiate herpes viral replication and oncolysis by complementing the function of genetic deletions intended to attenuate these viruses for safety.

In this study, we sought to determine the utility of oncolytic herpes viral therapy when delivered in combination with two currently used chemotherapeutic drugs for ATC: Adriamycin and paclitaxel. Paclitaxel has been shown to increase GADD34 mRNA expression in ovarian cancer cells (37). Adriamycin-induced DNA damage increases expression of the R2 protein of RR in colon cancer and the M2 portion of RR in osteosarcoma (31,38). We initially hypothesized that paclitaxel and Adriamycin might be able to enhance HSV-1 oncolysis through an up-regulation of GADD34 and RR in ATC cells.

Two well-studied, replication-competent, HSV-1 oncolytic viruses (G207 and NV1023) were selected for study. NV1023 is attenuated by the deletion of one copy of the $\gamma_1$34.5 neurovirulence gene, whereas G207 is attenuated by deletions in both copies of g134.5 and RR. Our cytotoxicity data showed synergy between the combination of G207 and paclitaxel using Chou-Talalay analyses. Interestingly, we observed antagonistic effects between Adriamycin and NV1023, whereas the other combinations of drug and virus were predominantly additive. The varied responses between these different combinations is an indicator of the complex interactions between a live virus relying on host cell machinery for replication and a toxic drug that induces cellular DNA damage (Adriamycin) or mitotic arrest (paclitaxel).

In focusing on interactions between G207 and paclitaxel, we sought to determine if G207 replication is affected by paclitaxel. One mechanism of anaplastic thyroid cancer resistance to paclitaxel is linked to activation of the Raf/MEK/ERK pathway (39). We found that phosphorylated MEK increases in a dose-dependent manner in KAT4 and DRO90-1cells treated with paclitaxel (data not shown). Because activated MEK may also enhance the replication of $\gamma_1$34.5-deleted HSV-1, we reasoned that G207 replication might be enhanced in either paclitaxel-treated or paclitaxel-resistant cells (40). However, G207 viral entry and proliferation studies in the presence of paclitaxel failed to show any enhancement of viral

replication. Viral entry was actually reduced by paclitaxel, and viral replication was either mildly impaired or unchanged with the addition of paclitaxel. These results are supported by a previous study showing that wild-type HSV-1(F strain) yield in Vero cells was reduced, although not completely inhibited, in the presence of paclitaxel (41). Another study showed that an ICP34.5-deleted modified oncolytic HSV-1exhibited additive or synergistic effects in breast cancer cell lines, although not through any alterations in viral replication (42). These findings suggest that synergistic cytotoxicity between G207 and paclitaxel is not related to any increase in G207 viral replication, in contrast to other viral and chemotherapy combinations (26–28).

To further assess these interactions, we explored how G207 in combination with paclitaxel might affect the mechanisms of paclitaxel therapeutic activity. During mitosis, the duplicated chromatids of a cell are separated to opposing poles by microtubules before cell cleavage. Dynamic changes in microtubule structure at mitotic spindles are critical for successful mitosis (33,43). Paclitaxel is known to stabilize microtubules, impairing such dynamic changes, impeding chromatid separation, blocking cell mitosis, and promoting apoptosis in malignant cells (32,33,36). We found that anaplastic thyroid cancer cells treated with G207 in combination with paclitaxel exhibited significant increases in measures of microtubule inhibition. For combination treatment, we detected enhanced microtubule acetylation (a marker of microtubule stabilization), mitotic arrest, inhibition of anaphase progression, and apoptosis compared with either single agent alone or untreated control samples. Wild-type HSV-1has evolved a mechanism of preventing host cell apoptosis for the purpose of promoting viral replication (44). However, some attenuated, oncolytic HSVs have been shown to induce apoptosis in some adjacent cancer cells not directly infected by the virus, potentially through a secreted viral protein (45). We detected apoptosis in a small percentage of KAT4 cells treated with G207 alone. The addition of G207 to paclitaxel, however, seemed to significantly enhance the apoptotic effects of paclitaxel therapy. These findings suggest that G207 might enhance the mechanisms of paclitaxel activity rather than vice versa, as originally hypothesized.

There is a mechanism to potentially account for these observations. Interestingly, an HSV-1 tegument protein, VP22, has been shown to be able to potently stabilize intracellular microtubule networks of infected cells (46). VP22 can reorganize microtubules in bundles and cause a high degree of microtubule stabilization. Elliott and colleagues treated Vero cells with HSV-1at MOI of 10 and found increased acetylation of microtubules 14 h after infection (46). Stabilized microtubule bundles were highly resistant to microtubule-depolymerizing agents and cold temperatures. VP22 has also been shown to possess an ability to efficiently spread from cell to cell through a Golgi-independent mechanism and has been hypothesized to potentiate cells to HSV infection by an unknown mechanism (47). Our data shows that low-dose G207 infection is insufficient alone to significantly inhibit cell proliferation and induce apoptosis through such a mechanism. However, we speculate that VP22 production from G207 infection may augment paclitaxel activity and may induce synergistic effects in microtubule stabilization, mitotic arrest, and apoptosis. Paclitaxel can enhance VP22-induced microtubule bundling, and truncated VP22 mutants have been used to isolate the domains necessary for this activity (48). It remains unclear as to why G207 and paclitaxel exhibit such synergistic effects but not NV1023 in combination with paclitaxel. It is possible that differences in viral strain and mechanisms of attenuation through genetic insertions and deletions may account for differences in interactive effects between these two oncolytic HSVs and paclitaxel.

The utility of G207 and paclitaxel combination therapy was corroborated in vivo in a murine flank tumor model of anaplastic thyroid cancer. Combination therapy was more effective than either treatment alone, and significant inhibition of tumor volume progression was noted in the combination-treated animals for the study duration. Furthermore, we did not observe any

toxicity in any of the treatment groups. These findings suggest that the combined application of G207 with paclitaxel might have significant clinical relevance.

Anaplastic thyroid cancer is a fatal disease for which current therapies are ineffective. Although paclitaxel is one of the few chemotherapeutic agents with some biological activity against ATC, as a single-agent therapy, it has failed to make a significant effect in improving patient survival. Replication-competent, attenuated, oncolytic herpes viruses possess activity against ATC (16,29). This study shows that the combination of G207 with paclitaxel has synergistic cytotoxic effects. G207 acts mainly through direct viral oncolysis, whereas paclitaxel acts through inhibition of mitosis and induction of apoptosis. We failed to show any increase in G207 viral entry or viral proliferation in ATC cells in the presence of paclitaxel. However, we did identify significantly increased microtubule acetylation, mitotic arrest, inhibition of metaphase to anaphase progression, aberrant mitotic chromosomal morphology, and apoptosis for combination treatment of G207 and paclitaxel. The prior identification of VP22, an HSV-1tegument protein, as a potent microtubule stabilizer allows for speculation that G207 may enhance paclitaxel effects through VP22 expression. This work offers a novel finding: combination oncolytic HSV and paclitaxel therapy may interact synergistically and enhance mechanisms of paclitaxel activity. These findings contrast with prior studies showing that DNA-damaging chemotherapies enhance oncolytic HSV replication through GADD34 and RR up-regulation. These results also suggest that the combination of G207 and paclitaxel may have utility for patients with anaplastic thyroid cancer and encourage the study of this regimen for clinical application.

Acknowledgments

Grant support: Flight Attendant Medical Research Institute, American College of Surgeons, and American Head and Neck Society (R.J.Wong). The costs of publication of this article were defrayed in part by the payment of page charges.This article must therefore be hereby marked advertisement in accordance with 18 U.S.C. Section 1734 solely to indicate this fact.

References

1. Green LD, Mack L, Pasieka JL. Anaplastic thyroid cancer and primary thyroid lymphoma: a review of these rare thyroid malignancies. J Surg Oncol 2006;94:725–736. [PubMed: 17131397]
2. Gilliland FD, Hunt WC, Morris DM, Key CR. Prognostic factors for thyroid carcinoma. A population-based study of 15,698 cases from the Surveillance, Epidemiology and End Results (SEER) program 1973–1991. Cancer 1997;79:564–573. [PubMed: 9028369]
3. Kebebew E, Greenspan FS, Clark OH, Woeber KA, McMillan A. Anaplastic thyroid carcinoma. Treatment outcome and prognostic factors. Cancer 2005;103:1330–1335. [PubMed: 15739211]
4. Shimaoka K, Schoenfeld DA, DeWys WD, Creech RH, DeConti R. A randomized trial of doxorubicin versus doxorubicin plus cisplatin in patients with advanced thyroid carcinoma. Cancer 1985;56:2155–2160. [PubMed: 3902203]
5. Williams SD, Birch R, Einhorn LH. Phase II evaluation of doxorubicin plus cisplatin in advanced thyroid cancer: a Southeastern Cancer Study Group Trial. Cancer Treat Rep 1986;70:405–407. [PubMed: 3955552]
6. Ain KB, Egorin MJ, DeSimone PA. Treatment of anaplastic thyroid carcinoma with paclitaxel: phase 2 trial using ninety-six-hour infusion. Collaborative Anaplastic Thyroid Cancer Health Intervention Trials (CATCHIT) Group.Thyroid 2000;10:587–594.
7. Nilsson O, Lindeberg J, Zedenius J, et al. Anaplastic giant cell carcinoma of the thyroid gland: treatment and survival over a 25-year period. World J Surg 1998;22:725–730. [PubMed: 9606289]
8. Mitchell G, Huddart R, Harmer C. Phase II evaluation of high dose accelerated radiotherapy for anaplastic thyroid carcinoma. Radiother Oncol 1999;50:33–38. [PubMed: 10225555]
9. McIver B, Hay ID, Giuffrida DF, et al. Anaplastic thyroid carcinoma: a 50-year experience at a single institution. Surgery 2001;130:1028–1034. [PubMed: 11742333]

10. Tennvall J, Lundell G, Wahlberg P, et al. Anaplastic thyroid carcinoma: three protocols combining doxorubicin, hyperfractionated radiotherapy and surgery. Br J Cancer 2002;86:1848–1853. [PubMed: 12085174]
11. Martuza RL, Malick A, Markert JM, Ruffner KL, Coen DM. Experimental therapy of human glioma by means of a genetically engineered virus mutant. Science 1991;252:854–856. [PubMed: 1851332]
12. Mineta T, Rabkin SD, Yazaki T, Hunter WD, Martuza RL. Attenuated multi-mutated herpes simplex virus-1 for the treatment of malignant gliomas. Nat Med 1995;1:938–943. [PubMed: 7585221]
13. Kooby DA, Carew JF, Halterman MW, et al. Oncolytic viral therapy for human colorectal cancer and liver metastases using a multi-mutated herpes simplex virus type-1 (G207). FASEB J 1999;13:1325–1334. [PubMed: 10428757]
14. Wong RJ, Kim SH, Joe JK, Shah JP, Johnson PA, Fong Y. Effective treatment of head and neck squamous cell carcinoma by an oncolytic herpes simplex virus. J Am Coll Surg 2001;193:12–21. [PubMed: 11442249]
15. Wong RJ, Patel SG, Kim SH, et al. Cytokine gene transfer enhances herpes oncolytic therapy in murine squamous cell carcinoma. Hum Gene Ther 2001;12:253–265. [PubMed: 11177562]
16. Yu Z, Eisenberg DP, Singh B, Shah JP, Fong Y, Wong RJ. Treatment of aggressive thyroid cancer with an oncolytic herpes virus. Int J Cancer 2004;112:525–532. [PubMed: 15382081]
17. Reid V, Yu Z, Schuman T, et al. Herpes oncolytic therapy of salivary carcinomas. Int J Cancer 2008;122:202–208. [PubMed: 17764117]
18. Wong RJ, Joe JK, Kim SH, Shah JP, Horsburgh B, Fong Y. Oncolytic herpes virus effectively treats murine squamous cell carcinoma and spreads by natural lymphatics to sites of lymphatic metastases. Hum Gene Ther 2002;13:1213–1223. [PubMed: 12133274]
19. Markert JM, Medlock MD, Rabkin SD, et al. Conditionally replicating herpes simplex virus mutant, G207 for the treatment of malignant glioma: results of a phase I trial. Gene Ther 2000;7:867–874. [PubMed: 10845725]
20. Rampling R, Cruickshank G, Papanastassiou V, et al. Toxicity evaluation of replication-competent herpes simplex virus (ICP 34.5 null mutant 1716) in patients with recurrent malignant glioma. Gene Ther 2000;7:859–866. [PubMed: 10845724]
21. Kemeny N, Brown K, Covey A, et al. Phase I, open label, dose-escalating study of a genetically engineered herpes simplex virus, NV1020, in subjects with metastatic colorectal carcinoma to the liver. Hum Gene Ther 2006;17:1214–1224. [PubMed: 17107303]
22. Chahlavi A, Todo T, Martuza RL, Rabkin SD. Replication-competent herpes simplex virus vector G207 and cisplatin combination therapy for head and neck squamous cell carcinoma. Neoplasia 1999;1:162–169. [PubMed: 10933051]
23. Toyoizumi T, Mick R, Abbas AE, Kang EH, Kaiser LR, Molnar-Kimber KL. Combined therapy with chemotherapeutic agents and herpes simplex virus type 1 ICP34.5 mutant (HSV-1716) in human non-small cell lung cancer. Hum Gene Ther 1999;10:3013–3029. [PubMed: 10609661]
24. Nawa A, Nozawa N, Goshima F, et al. Oncolytic viral therapy for human ovarian cancer using a novel replication-competent herpes simplex virus type I mutant in a mouse model. Gynecol Oncol 2003;91:81–88. [PubMed: 14529666]
25. Cinatl J Jr, Cinatl J, Michaelis M, et al. Potent oncolytic activity of multimutated herpes simplex virus G207 in combination with vincristine against human rhabdomyosarcoma. Cancer Res 2003;63:1508–1514. [PubMed: 12670897]
26. Petrowsky H, Roberts GD, Kooby DA, et al. Functional interaction between fluorodeoxyuridine induced cellular alterations and replication of a ribonucleotide reductase-negative herpes simplex virus. J Virol 2001;75:7050–7058. [PubMed: 11435585]
27. Bennett JJ, Adusumilli P, Petrowsky H, et al. Upregulation of GADD34 mediates the synergistic anticancer activity of mitomycin C and a g134.5 deleted oncolytic herpes virus (G207). FASEB J 2004;18:1001–1003. [PubMed: 15059970]
28. Aghi M, Rabkin S, Martuza RL. Effect of chemotherapy-induced DNA repair on oncolytic herpes simplex viral replication. J Natl Cancer Inst 2006;98:38–50. [PubMed: 16391370]
29. Huang YY, Yu Z, Lin SF, Li S, Fong Y, Wong RJ. Nectin-1is a marker of thyroid cancer sensitivity to herpes oncolytic therapy. J Clin Endocrinol Metab 2007;92:1965–1970. [PubMed: 17327376]

30. Tewey KM, Rowe TC, Yang L, Halligan BD, Liu LF. Adriamycin-induced DNA damage mediated by mammalian DNA topoisomerase II. Science 1984;226:466–468. [PubMed: 6093249]

31. Lin ZP, Belcourt MF, Cory JG, Sartorelli AC. Stable suppression of the R2 subunit of ribonucleotide reductase by R2-targeted short interference RNA sensitizes p53(−/−) HCT-116 colon cancer cells to DNA-damaging agents and ribonucleotide reductase inhibitors. J Biol Chem 2004;279:27030–27038. [PubMed: 15096505]

32. Jordan MA, Wendell K, Gardiner S, Derry WB, Copp H, Wilson L. Mitotic block induced in HeLa cells by low concentrations of paclitaxel (Taxol) results in abnormal mitotic exit and apoptotic cell death. Cancer Res 1996;56:816–825. [PubMed: 8631019]

33. Jordan MA, Wilson L. Microtubules as a target for anticancer drugs. Nat Rev Cancer 2004;4:253–265. [PubMed: 15057285]

34. Chou TC. Theoretical basis, experimental design, and computerized simulation of synergism and antagonism in drug combination studies. Pharmacol Rev 2006;58:621–681. [PubMed: 16968952]

35. Piperno G, LeDizet M, Chang XJ. Microtubules containing acetylated a-tubulin in mammalian cells in culture. J Cell Biol 1987;104:289–302. [PubMed: 2879846]

36. Kelling J, Sullivan K, Wilson L, Jordan MA. Suppression of centromere dynamics by Taxol in living osteosarcoma cells. Cancer Res 2003;63:2794–2801. [PubMed: 12782584]

37. Sugimura M, Sagae S, Ishioka S, Nishioka Y, Tsukada K, Kudo R. Mechanisms of paclitaxel-induced apoptosis in an ovarian cancer cell line and its paclitaxel resistant clone. Oncology 2004;66:53–61. [PubMed: 15031599]

38. Fellenberg J, Dechant MJ, Ewerbeck V, Mau H. Identification of drug-regulated genes in osteosarcoma cells. Int J Cancer 2003;105:636–643. [PubMed: 12740912]

39. Pushkarev VM, Starenki DV, Saenko VA, et al. Molecular mechanisms of the effects of low concentrations of Taxol in anaplastic thyroid cancer cells. Endocrinology 2004;145:3143–3152. [PubMed: 15044368]

40. Smith KD, Mezhir JJ, Bickenbach K, et al. Activated MEK suppresses activation of PKR and enables efficient replication and in vivo oncolysis by Deltag(1)34.5 mutants of herpes simplex virus 1. J Virol 2006;80:1110–1120. [PubMed: 16414988]

41. Kotsakis A, Pomeranz LE, Blouin A, Blaho JA. Microtubule reorganization during herpes simplex virus type 1 infection facilitates the nuclear localization of VP22, a major virion tegument protein. J Virol 2001;75:8697–8711. [PubMed: 11507215]

42. Hu JC, Hallden G, Shorrock C, et al. Combination of a second generation genetically modified herpes simplex virus 1 (HSV1) with paclitaxel in the treatment of breast cancer in vitro. ASCO Annual Meeting Proceedings 2004;22(14S):723.

43. Rusan NM, Fagerstrom CJ, Yvon AM, Wadsworth P. Cell cycle-dependent changes in microtubule dynamics in living cells expressing green fluorescent protein a tubulin. Mol Biol Cell 2001;12:971–980. [PubMed: 11294900]

44. Galvan V, Roizman B. Herpes simplex virus 1 induces and blocks apoptosis at multiple steps during infection and protects cells from exogenous inducers in a cell type-dependent manner. Proc Natl Acad Sci U S A 1998;95:3931–3936. [PubMed: 9520470]

45. Stanziale SF, Petrowsky H, Adusumilli PS, Ben-Porat L, Gonen M, Fong Y. Infection with oncolytic herpes simplex virus-1 induces apoptosis in neighboring human cancer cells: a potential target to increase anticancer activity. Clin Cancer Res 2004;10:3225–3232. [PubMed: 15131064]

46. Elliott G, O'Hare P. Herpes simplex virus type 1 tegument protein VP22 induces the stabilization and hyperacetylation of microtubules. J Virol 1998;72:6448–6455. [PubMed: 9658087]

47. Elliott G, O'Hare P. Intercellular trafficking and protein delivery by a herpes virus structural protein. Cell 1997;88:223–233. [PubMed: 9008163]

48. Martin A, O'Hare P, McLauchlan J, Elliott G. Herpes simplex virus tegument protein VP22 contains overlapping domains for cytoplasmic localization, microtubule interaction, and chromatin binding. J Virol 2002;76:4961–4970. [PubMed: 11967313]

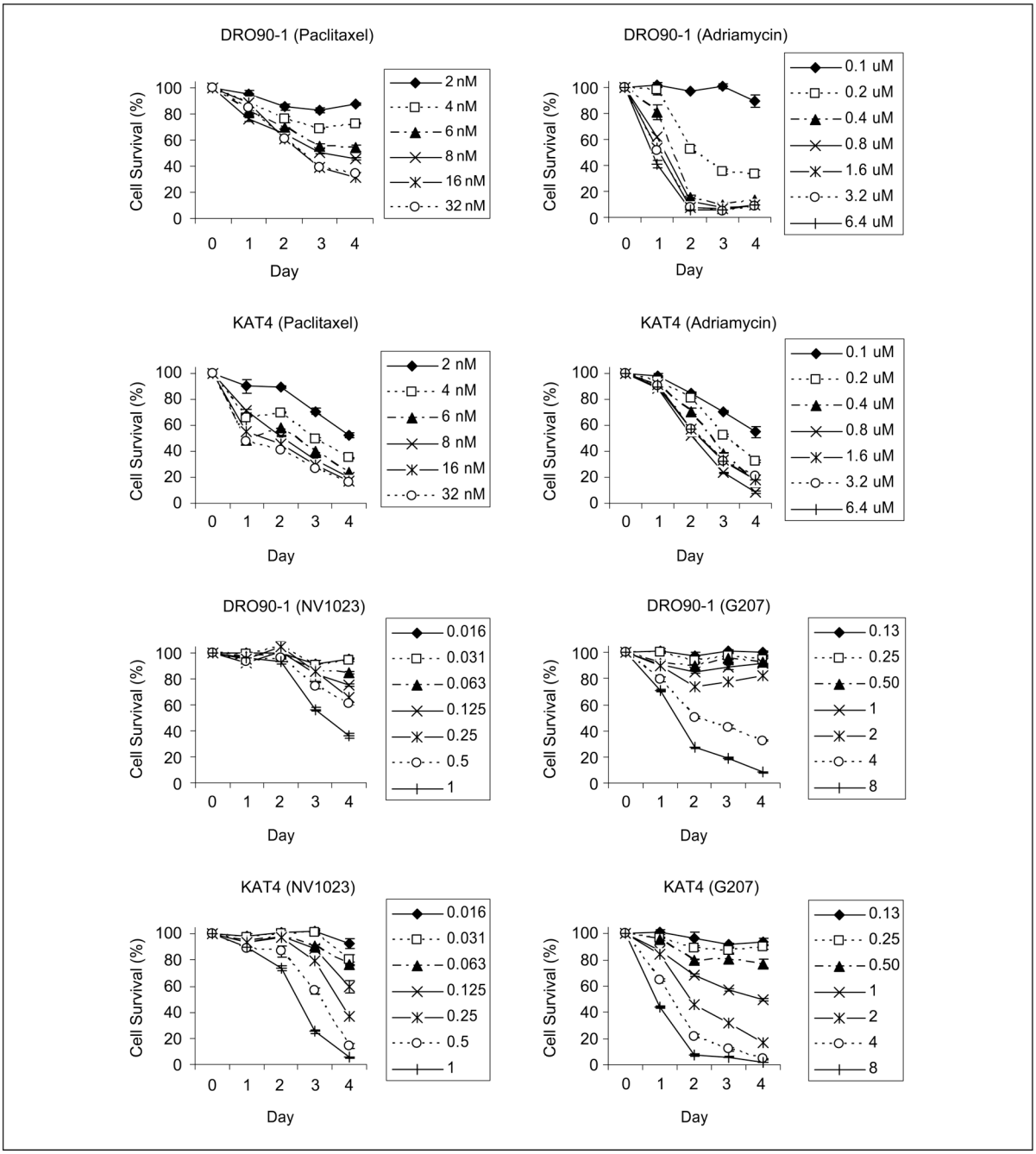

Fig. 1.

Time course cytotoxicity assays of paclitaxel, Adriamycin, NV1023, and G207 on the anaplastic thyroid cancer cell lines KAT4 and DRO90-1. A range of serial dilutions was studied to identify optimal viral dosing and drug concentrations.The percentage of surviving cells *in vitro* was determined by LDH assays, considering control samples to be 100% viable. Points, mean of triplicate samples; bars, SE.

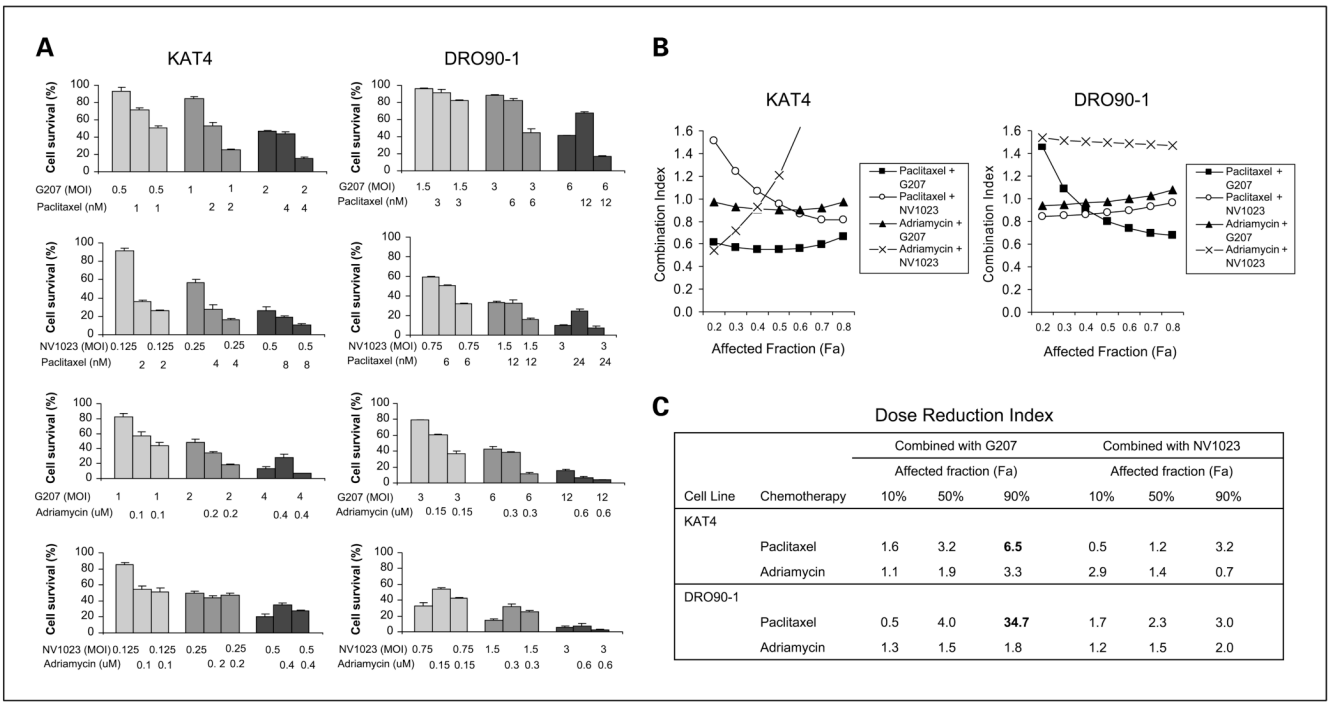

Cell Line	Chemotherapy	Combined with G207 Affected fraction (Fa) 10%	50%	90%	Combined with NV1023 Affected fraction (Fa) 10%	50%	90%
KAT4							
	Paclitaxel	1.6	3.2	**6.5**	0.5	1.2	3.2
	Adriamycin	1.1	1.9	3.3	2.9	1.4	0.7
DRO90-1							
	Paclitaxel	0.5	4.0	**34.7**	1.7	2.3	3.0
	Adriamycin	1.3	1.5	1.8	1.2	1.5	2.0

Fig. 2.

Cytotoxicity of combination herpes oncolytic virus and chemotherapy. *A*, cytotoxic effects of G207 or NV1023 in combination with the paclitaxel or doxorubicin on KAT4 and DRO90-1on cell survival using LDH assays *in vitro*.Varying viral and drug concentrations were applied alone or in combination for a 4-d exposure period. G207 plus paclitaxel showed enhanced cytotoxic effects.The combinations of G207 plus Adriamycin and NV1023 plus paclitaxel showed predominantly additive cytotoxic effects for both cell lines. The combination of NV1023 plus Adriamycin failed to result in additive cytotoxic effects for either KAT4 or DRO90-1. Columns, mean; bars, SE. *B*, the CIs of G207 or NV1023 in combination with paclitaxel or Adriamycin were calculated using Chou-Talalay analyses and plotted against the affected fraction (*Fa*) or the percentage of cell death resulting from combined therapy. CI of <0.9 indicates synergy, CI between 0.9 and 1.1is addictive, and CI of >1.1indicates antagonism. Paclitaxel and G207 show synergistic effects for KAT4 and at higher affected fractions of DRO90-1. In contrast, Adriamycin and NV1023 exhibit antagonistic effects together, whereas other combinations of drug and virus were predominantly additive. *C*, the dose reduction index (*DRI*) was calculated for each drug and virus combination at various affected fractions. The dose reduction index was greatest for paclitaxel with G207 for both KAT4 and DRO90-1cell lines at an affected fraction of 90%.

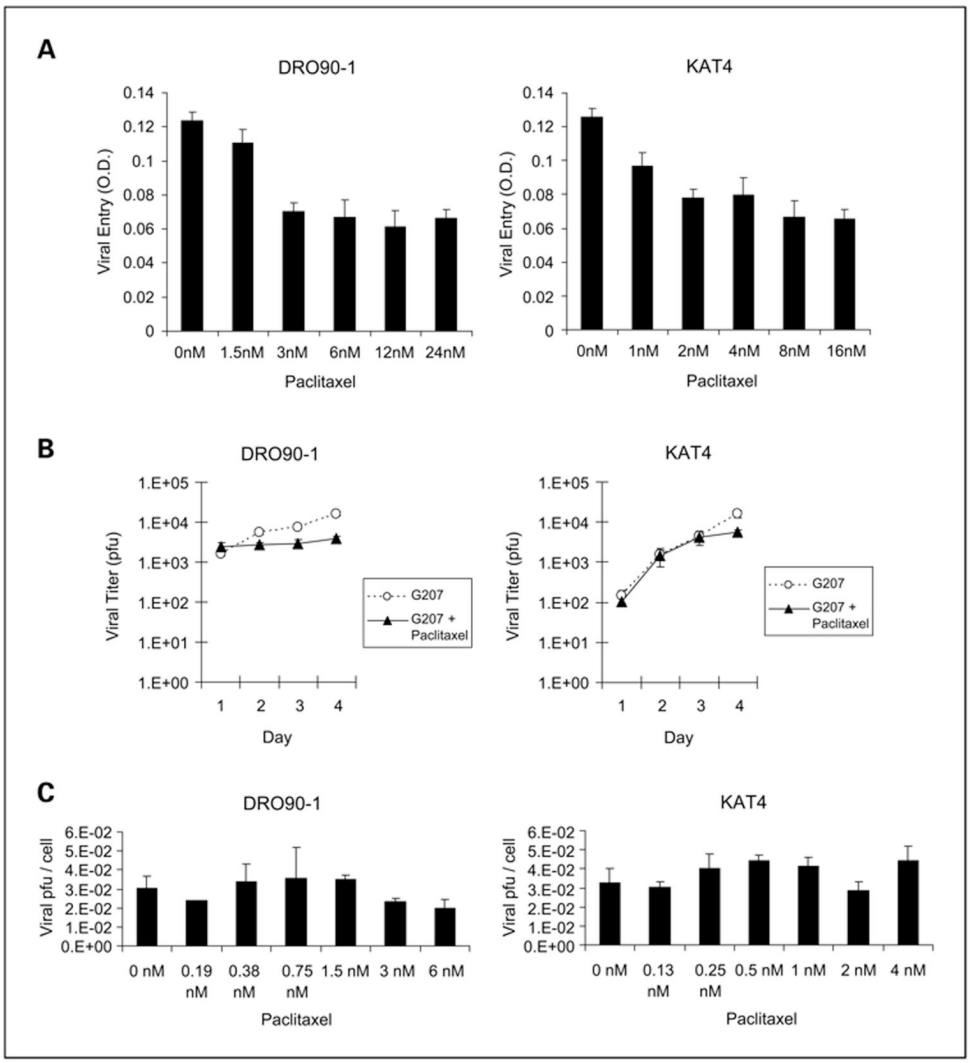

Fig. 3.

Paclitaxel fails to increase G207 viral entry or viral proliferation. *A*, measures of G207 viral entry and early gene expression assessed by *lacZ* assays in ATC cell lines show modest but significant decreases with low-dose paclitaxel and stable effects at doses higher than 2 nmol/L. *B*, total G207 viral proliferation per well was measured after exposure of ATC cells to G207 atMOI of 0.5 (KAT4) orMOI of 1.5 (DRO90-1) in combination with paclitaxel at 1nmol/L (KAT4) or 3 nmol/L (DRO90-1).Viral titers were calculated daily by plaque assays, and the number of recovered pfu was assessed. The combination of paclitaxel with G207 slightly impaired viral replication compared with G207 alone in DRO90-1cells and was not affected in KAT4 cells. *C*, G207 viral proliferation was measured in combination with a range of paclitaxel concentrations at 48 h after exposure to G207 atMOI of 1. Recovered viral pfu were adjusted per viable cell number to account for varying cytotoxic effects. There were no significant differences in the amount of recovered G207 per viable cell with or without the addition of paclitaxel at doses up to 6 nmol/L. Columns, mean; bars, SE.

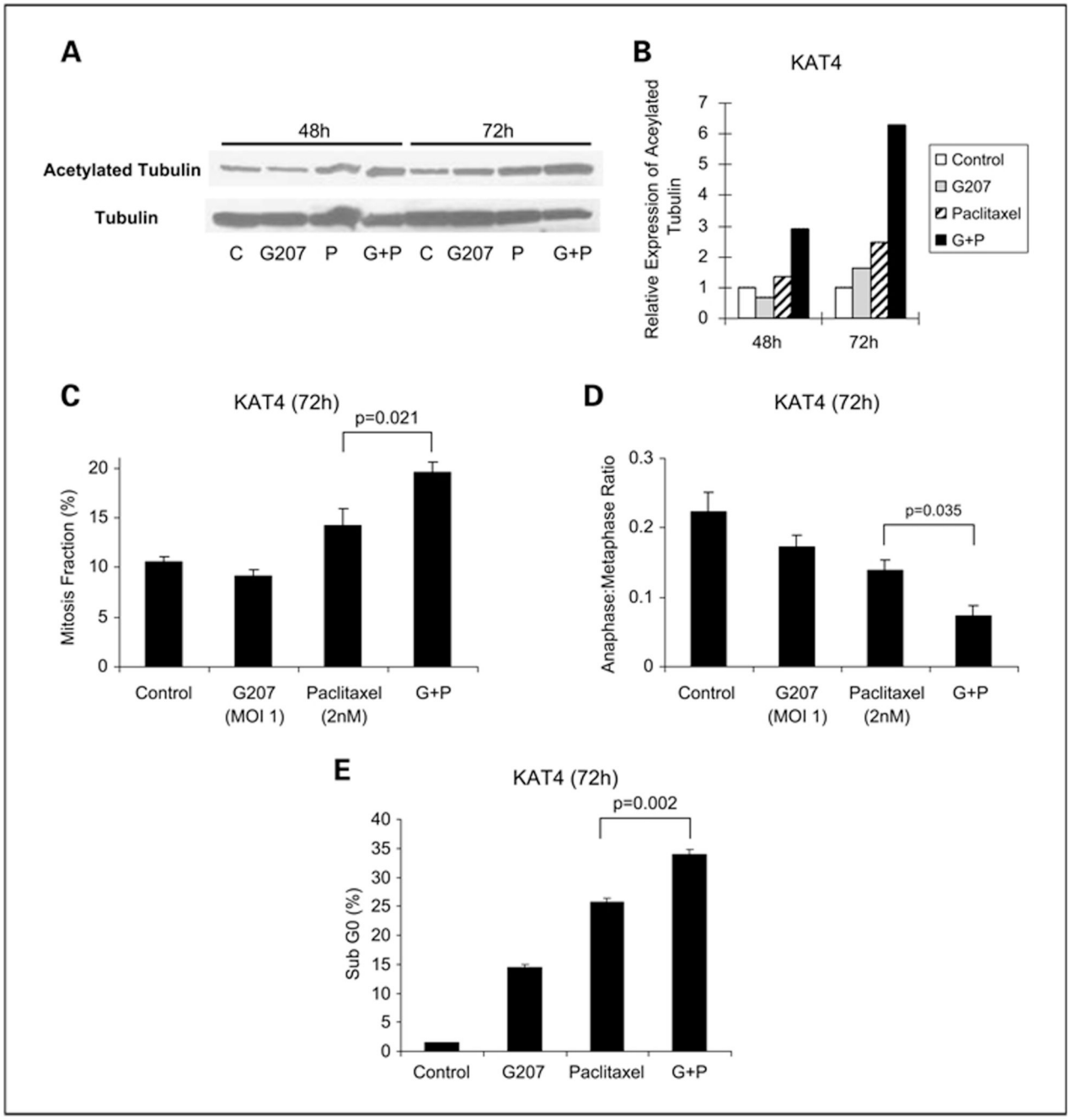

Fig. 4.

G207 enhances mechanisms of paclitaxel activity. *A*, KAT4 cells were treated with G207 (MOI, 1) and/or paclitaxel (2 nmol/L) or vehicle (control) for 48 or 72 h. Acetylated α-tubulin and α-tubulin were assessed by Western blot. *B*, band densities were quantified, and the ratio of acetylated α-tubulin to α-tubulin was determined. At 72 h, G207 alone slightly increased α-tubulin acetylation (ratio of 1.61) compared with control (ratio of 1). Paclitaxel alone yielded a ratio of 2.45. The combination of G207 and paclitaxel increased the ratio of acetylated α-tubulin to 6.29. *C*, the percentage of KAT4 cells in mitosis was assessed after treatment with G207 (MOI, 1) or paclitaxel (2 nmol/L) for 72 h. Cells were stained with α-tubulin antibodies and DAPI and evaluated by immunofluorescence confocal microscopy. A minimum of 1,500

cells were counted from at least five different fields for each condition. A significant increase in the percentage of cells arrested in mitosis was detected for the combination of paclitaxel with G207 compared with other conditions. *D*, the ratio of cells in anaphase/metaphase as determined by confocal microscopy showed a significant decrease for the combination of paclitaxel and G207 compared with other conditions. *E*, the percentage of cells in apoptosis was assessed by staining with propidium iodide, fluorescence-activated cell sorting analysis, and determination of the sub-G_0 fraction. A significant increase in the percentage of apoptotic cells for combination of G207 and paclitaxel treatment was detected. Columns, mean for triplicate samples; bars, SE.

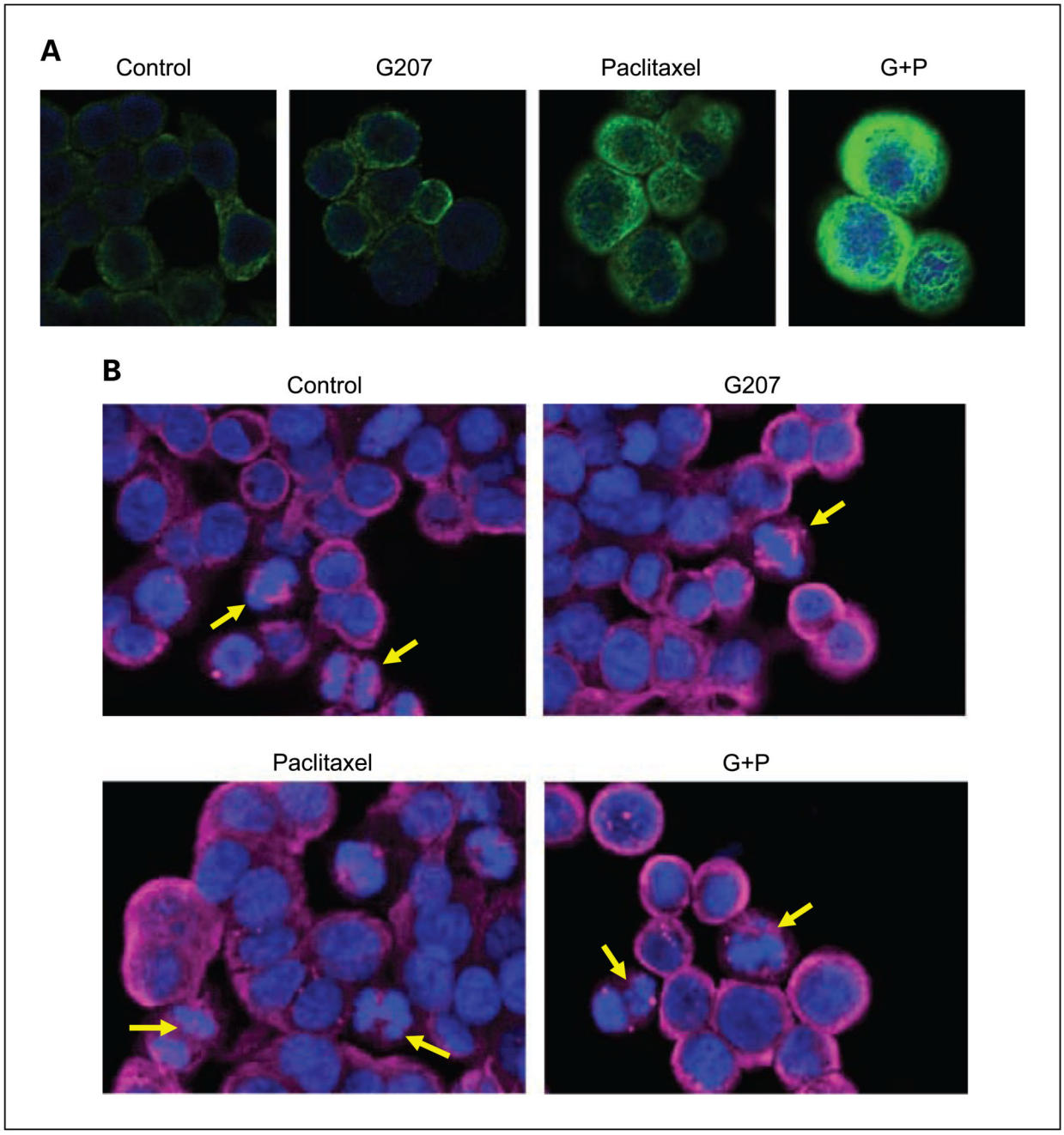

Fig. 5.

Immunofluorescence confocal microscopy. *A*, KAT4 cells stained with fluorescent antibodies to acetylated α-tubulin (*green*) andDAPI (*blue*) show increased acetylated α-tubulin after treatment with G207 (MOI,1) and paclitaxel (2 nmol/L) compared with single-agent treatment or control cells. *B*, KAT4 cells were stained with fluorescent antibodies to α-tubulin (*red*) andDAPI (*blue*) 72 h after treatment with G207 (MOI, 1), paclitaxel (2 nmol/L), both in combination, or vehicle. Both control-treated and G207-treated cells showed normal chromosomal morphology and metaphase alignment.The sister chromatids are drawn apart uniformly by microtubules to opposing poles during anaphase (*yellow arrows*). Some paclitaxel-treated cells showed a failure by some chromosomes to congregate linearly along

the metaphase plate, with others migrating in an aberrant fashion toward the opposing poles (*yellow arrows*). Cells treated by the combination of G207 and paclitaxel exhibited aberrant chromosomal morphology, fragmented chromosomes (*yellow arrows*), and mitotic catastrophes.

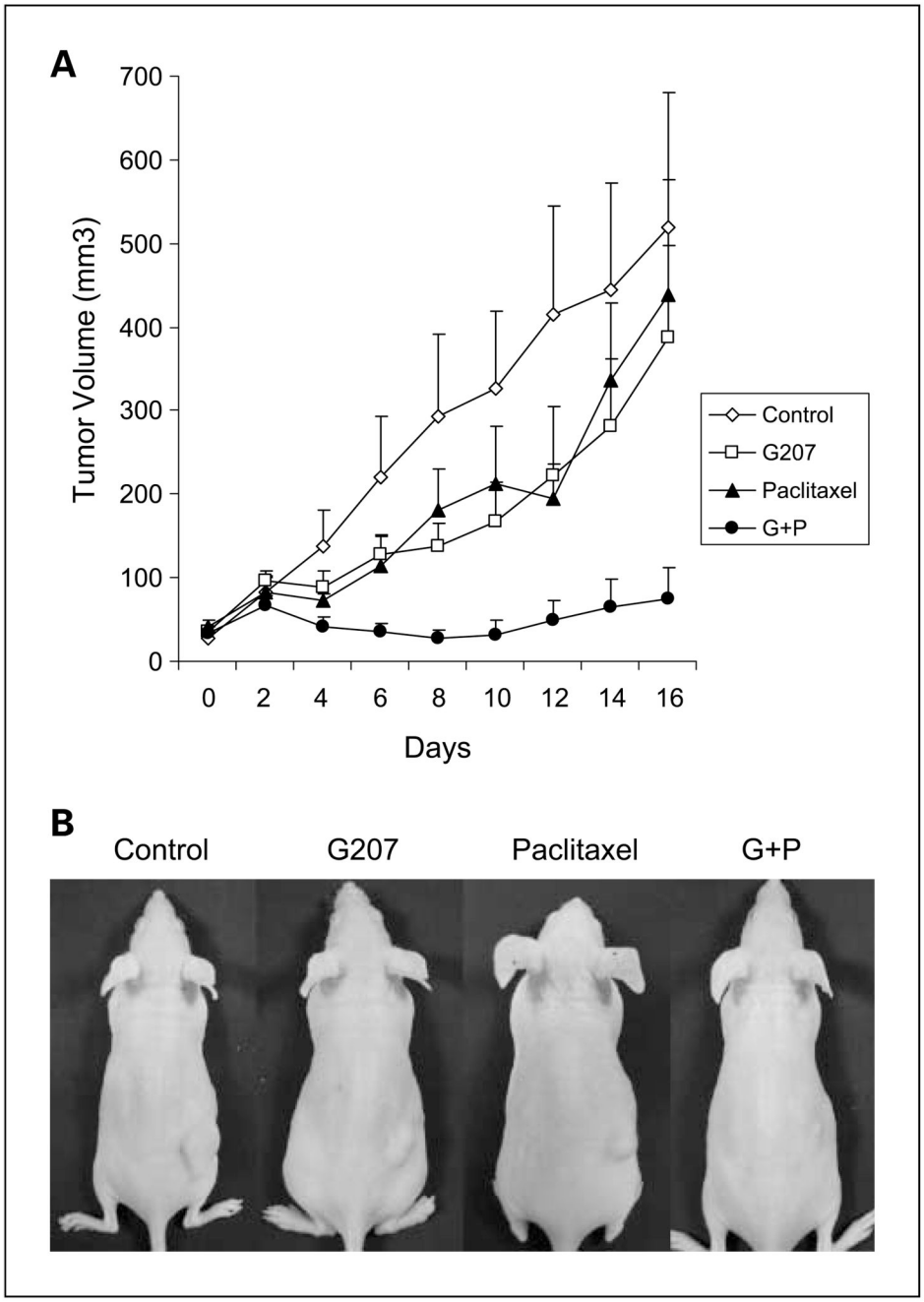

Fig. 6.

Combination of single G207 and biweekly paclitaxel therapy *in vivo* in a murine xenograft flank tumor model. *A*, KAT4 flank tumors were established in nude mice and treated with vehicle (PBS i.t. + cremphor EL mixture i.p.), G207 (2×10^7 pfu i.t. + cremphor EL mixture i.p.), paclitaxel (0.4 mg i.p. + PBS i.t.), or both G207 and paclitaxel in combination (2×10^7 pfu i.t. + 0.4 mg i.p.).Tumor volumes were significantly lower for mice treated with combination therapy compared with single modality treatment or control. *B*, representative animals 16 d after treatment show significant tumor volume differences. There were no significant differences in the mean body weight of experimental groups, and no morbidity observed was attributable to therapy with G207, paclitaxel, or both in combination.